Acta Polytechnica CTU Proceedings **40**:111–116, 2023
https://doi.org/10.14311/APP.2023.40.0111

Published by the Czech Technical University in Prague

GENERATION OF LDPM STRUCTURE FORMED BY VORONOI CELLS

Jan Vozáb*, Jan Vorel

Czech Technical University in Prague, Faculty of Civil Engineering, Department of Mechanics, Thákurova 7, 166 29 Prague 6, Czech Republic

* corresponding author: jan.vozab@fsv.cvut.cz

Abstract. A preliminary study of an approach to internal structure generation used in lattice discrete particle models (LDPMs) [1]. The presented method used for particle generation and placement is intended to help realistically capture the internal structure of materials. First, a method for structure generation using LDPM is presented. Then, the method of particle generation using a Voronoi diagram [2] is described. The last part is the optimizations on the algorithm that use Apollonius circles to calculate the specific points of the Voronoi diagram.

Keywords: LDPM, Voronoi diagram, Voronoi cell, internal structure.

1. Introduction

The use of composite materials such as reactoplasts is increasingly common in today's industry. The construction industry is no exception. However, other industries such as aerospace or automotive differ in several important ways. This mainly concerns the degree of material curing at which these materials begin to load. This effect has a strong influence on the response of the material under load, especially in combination with viscoelasticity. At the same time, the material properties change over time.

One of the structural elements used in construction where these materials are involved involves chemical anchors. Particle-filled polymers act as a mortar binder layer between the anchor and the building element to which they are attached. These mortars are considered as homogeneous materials. But at lower scales, they can be characterized as heterogeneous materials [3]. In [4], is described that the modification of conventional continuum models (phase-field and peridynamic) is not possible without discretizing the internal structure. For this reason we decided to use a discrete model. Figure 1 shows the real internal structure of such a polymer mortar. The polymer binder that connects the grains is shown in gray and shown in light color. It is clearly shown that the grains are of different sizes. The failure of these materials is mainly around the grains in the mortar [5, 6]. Breakage through the grains occurs mainly in high-strength concretes [1]. This allows us to use the Lattice Discrete Particle Model (LDPM), which creates the internal structure of the material. It is convenient for the materials we are investigating. The LDPM material model response is dependent on particle distribution, and thus multiple simulations are needed to provide credible results [7].

However, as can be seen in the Figure 1, most of the grains are not circular. The LDPM model only allows the generation of circular (2D) or spherical (3D) particles. Our goal is to modify the LDPM model to allow the generation of grains of different sizes and shapes. Therefore, we decided to modify the particle generation using a Voronoi diagram. The computational complexity of this model is also an important factor. This paper focuses on the modification of the algorithm and its subsequent optimization.

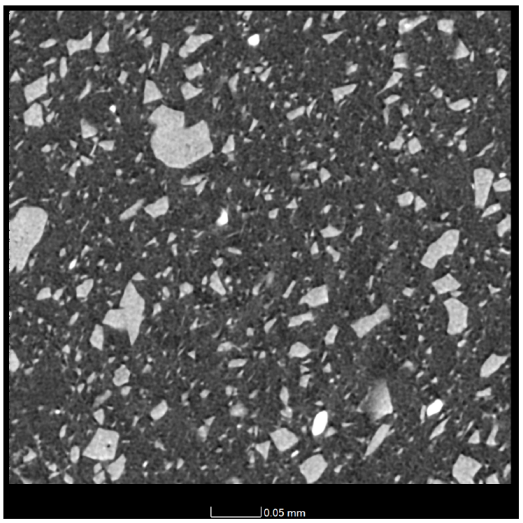

Figure 1. Detail of internal structure: Hilti HIT RE 500.

2. LDPM structure

First of all, it is important to describe the original method of generating the mesosctucture using the LDPM method [1]. We are given the sample geometry and the prescriptive gradation curve, i.e., the maximum and minimum aggregate size, as input for structure generation.

The maximum aggregate size defines the upper limit of the gradation curve. In contrast, the minimum aggregate size defines its lower boundary, i.e., the

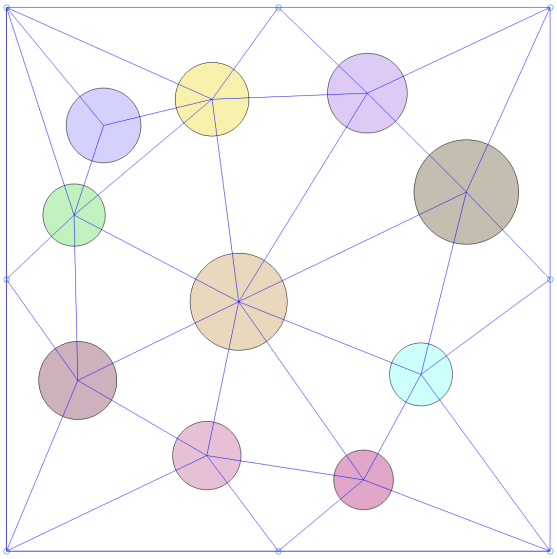

Figure 2. Delaunay triangulation result given set of particles.

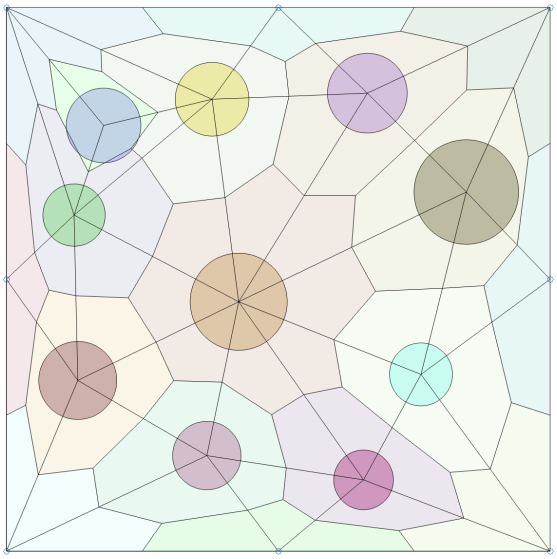

Figure 3. LDPM structure for circular particles.

diameter below which no discretized particles are generated and located. Thus, the minimum aggregate size affects the fineness of the discrete network and the computational cost.

The process begins with the generation of particles on the exterior of the sample. In our case (2D), points are first generated at the corners and then in the middle of the sides of the square. In the Figure 2 they are shown by the blue circular points. This is followed by particle generation on the interior of the sample. The particles are placed from largest to smallest in a random position to ensure that the sample contains as many as possible. In the figure, these particles are represented by circles of different colors. The nearest particles are then detected using Delaunyan triangulation, which results in the underlying polytopes in the given space. They represent triangles in the plane and tetrahedrons in space. In the Figure 2 they are shown

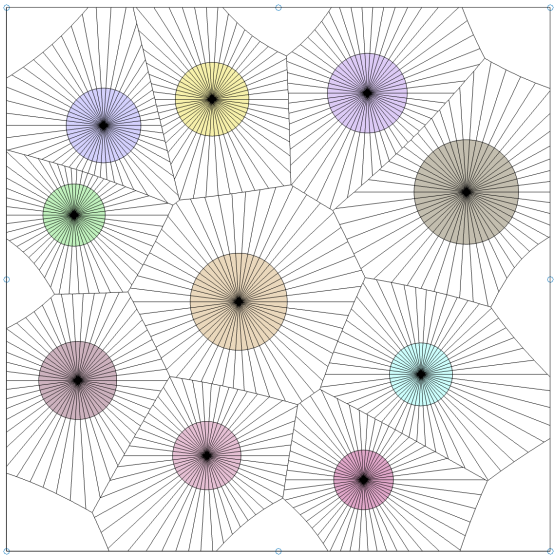

Figure 4. Structure of circular Voronoi particles before composition.

with blue lines connecting the individual particles. The following process divides the triangle into parts that belong to the particles that form its vertices. The centres of the sides and the centre of the triangle are calculated, and the part of the triangle is connected to the particle to which it belongs. The individual segments are then combined to form the resulting polyhedral cells (Figure 3). When all the polyhedral particles have been formed, their interaction with each other has to be determined through the facets formed by the splitting of the triangles. The displacements and rotations of these neighboring particles form the discrete compatibility equations in terms of rigid-body kinematics. On each facet of the cell, an inter-scale constitutive law is formulated to simulate cohesive fracture, compaction due to pore collapse, frictional slip, and velocity effect. Finally, equilibrium equations are formulated for each individual particle.

3. Voronoi structure

This article studies the potential use of Voronoi cell tessellation [2] for the LDPM model. The Voronoi cells are particles with a boundary representing half the distance between the particles from which tessellation occurs [8]. Boundaries in the fundamental case are represented by lines for points in 2D and planes for points in 3D. For different particles, the Voronoi cells are more complex. The simplest planar particles in the plane are circles. When the radii are equal, the boundary is represented by a straight line. When the radii differ, the boundary becomes curved. Considering more complex particles, such as ellipses, the boundary complexity becomes even greater. However, it is possible to generate a structure for particles of any shape.

In the Figure 4 you can see the cell structure created for the same set of particles as for the LDPM struc-

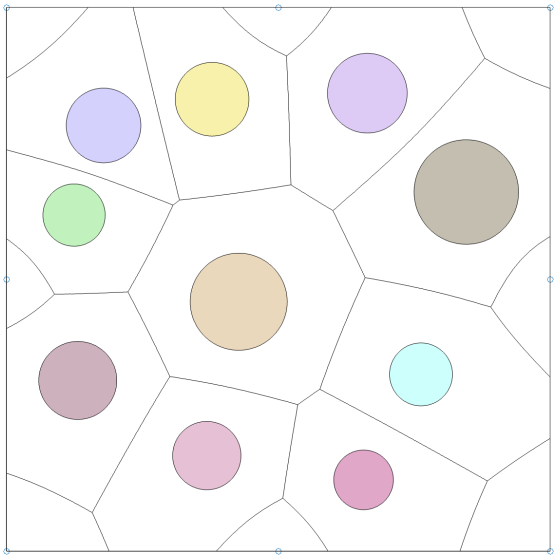

FIGURE 5. Structure of circular Voronoi particles after composition.

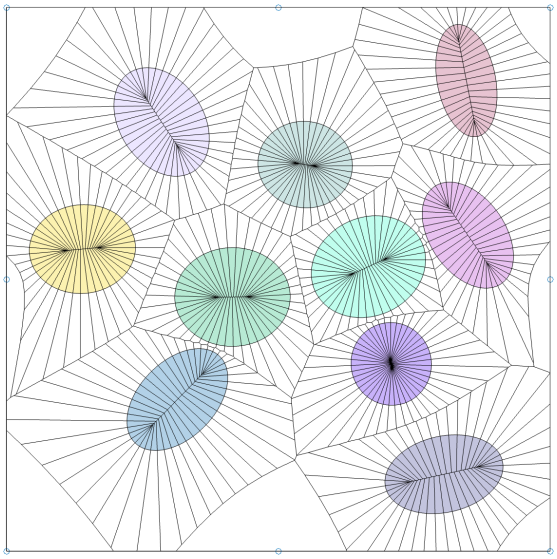

FIGURE 6. Structure of elliptical Voronoi particles before composition.

ture. The challenging thing about forming a structure using Voronoi cells is that if the particles have different radii, or if they are not circular, the boundary between them is formed by a curve. In the figure you can see that in particular, the boundaries of cells formed by particles on the perimeter of a square are curves. Furthermore, this effect can be seen for particles that are close together. We deal with this effect by generating more points on the boundary of the particle, thus generating a special cell. Once the entire structure is generated, the points belonging to each particle are merged into a complete cell that takes into account the size and shape of the particle. The resulting boundary is a semilinear curve. Result is shown in the Figure 5. In this case, the particles are represented by 50 points on the particle boundary. For the calculation we used the Matlab software [9]. Compared to the structure formed by the LDPM method, they are smoother. Smaller particles are connected to fewer other particles. At the same time, there are no fragments like those seen in the upper left corner of the picture. For the purple particle, the cell boundary passes through the particle itself.

The Figure 6 shows a structure made up of elliptical cells. At first glance, it is obvious that the boundaries between the particles are much more curved due to the complexity of the particle shape. Therefore, even when the particles are represented by 44 points, small fluctuations in the smoothness of the boundary can be seen. Nevertheless, in the Figure 7 the boundaries are as we would expect and do not contain any major fragments.

4. Optimization of the algorithm

Such a high number of points representing each particle would greatly affect the speed of the calculation. Therefore, we focused on how we could reduce the

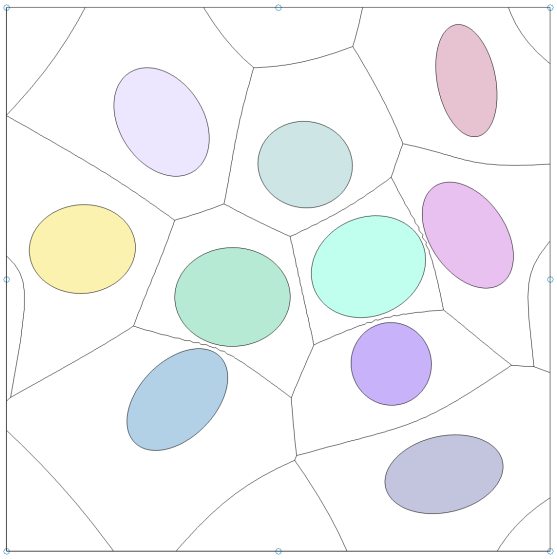

FIGURE 7. Structure of elliptical Voronoi particles after composition.

number of points on the particle boundary while maintaining the accuracy of the boundary. Therefore, we decided to see what effect replacing random points with specific points on the particle boundary. One of these characteristic points is the point of connection of the three cells. It is also the centre of the circle that touches the three cells. This problem is not trivial and is generally called the Apollonius problem or the Apollonius circle.

$$f(x,y) = (x - x_c)^2 + (y - y_c)^2 = r^2 \tag{1}$$

$$(x_s - x_{ci})^2 + (y_s - y_{ci})^2 = (r_s - s_i r_i)^2 \tag{2}$$

Equation (1) is general expression of circle, where x_c and y_c refers to the center of the circle and r is radius. The following Equation (2) represents the general solution of the Apollonius circle, where s_i

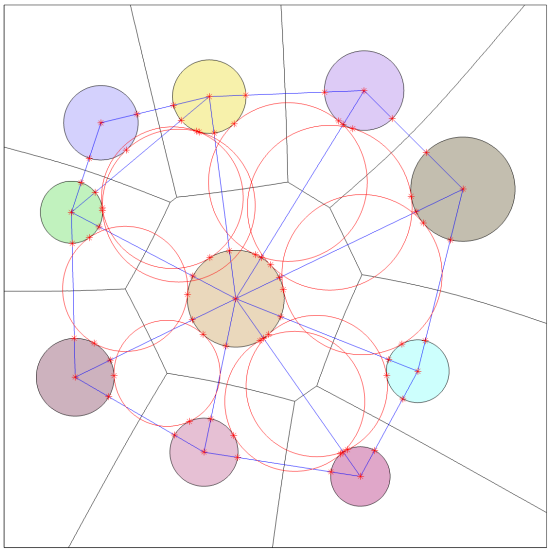

Figure 8. Apollonius circles connecting circular particles.

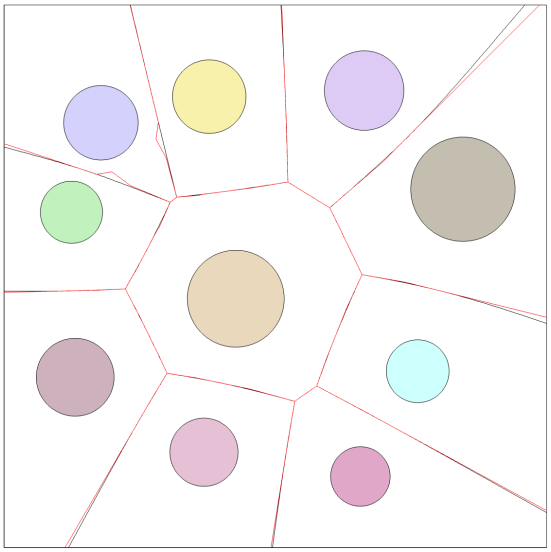

Figure 10. Optimized Voronoi structure of circular particles after composition.

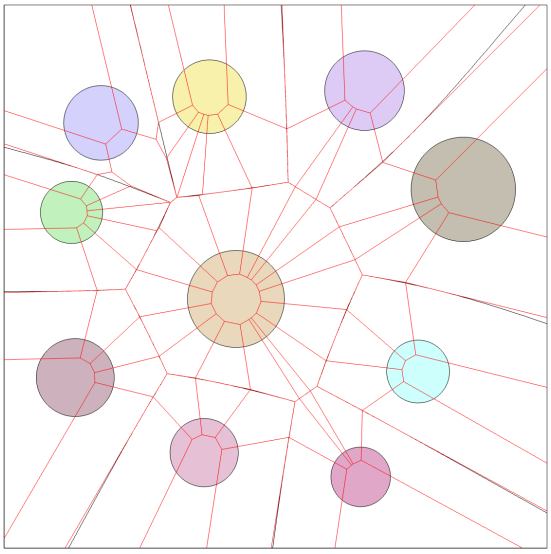

Figure 9. Optimized Voronoi structure of circular particles before composition.

is coefficient, that determines whether the resulting circle will be touched by the particle from the interior or the exterior.

The result of this system of equations can be seen in the Figure 8 for the same set of particles. The linkages between the particles are shown in blue. The red shows the circles between the particles as well as the points that these circles create in contact with particle The boundaries calculated by the unoptimized method are shown in black color. The Figure 9 shows the Voronoi diagram before composition. At first glance, one can see the much smaller number of cells of which it is composed. The Figure 10 shows the resulting structure after composition on the resulting cells. Small fragments can be seen where the cells are close together, or at the boundaries of the diagram when the particles have different radii. But the resulting structure is formed at an average of 8 points per particle. Even so, its accuracy is very consistent with the unoptimized method.

We have tried a similar approach to calculate points for ellipses. But we encountered the problem here that the general equation of the Apollonius circle is noticeably more complicated. With the general equation of the ellipse:

$$f(x,y) = \frac{((x-x_c)\cdot\cos\alpha + (y-y_c)\cdot\sin\alpha)^2}{a^2} + \frac{((x-x_c)\cdot\sin\alpha - (y-y_c)\cdot\cos\alpha)^2}{b^2} = 1, \tag{3}$$

which then has to be converted into the general equation of the conic section:

$$E(x,y) = ax^2 + 2bxy + cy^2 + 2dx + 2ey + f. \tag{4}$$

Then, following the procedure defined in [10], several parameters are calculated to form a determinant, which for a single ellipse is defined as a polynomial of degree 184. The resulting system of equations:

$$\Delta_1(xs,ys,s) = \Delta_2(xs,ys,s) = \Delta_3(xs,ys,s) = 0. \tag{5}$$

The resulting system of equations is a very challenging problem to solve. Therefore, we tried to come up with a modification that would make the calculation possible. So we took inspiration from the circle equation, and considered that the ellipses will grow with one parameter until they intersect at one point. From this assumption comes the equation together with the system of equations:

$$f_i(x,y,r) = \frac{((x-x_{ci})\cdot\cos\alpha_i + (y-y_{ci})\cdot\sin\alpha_i)^2}{(a_i+r)^2} + \frac{((x-x_{ci})\cdot\sin\alpha_i - (y-y_{ci})\cdot\cos\alpha_i)^2}{(b_i+r)^2} - 1 = 0, \tag{6}$$

$$f_1(x,y,r) = f_2(x,y,r) = f_3(x,y,r) = 0. \tag{7}$$

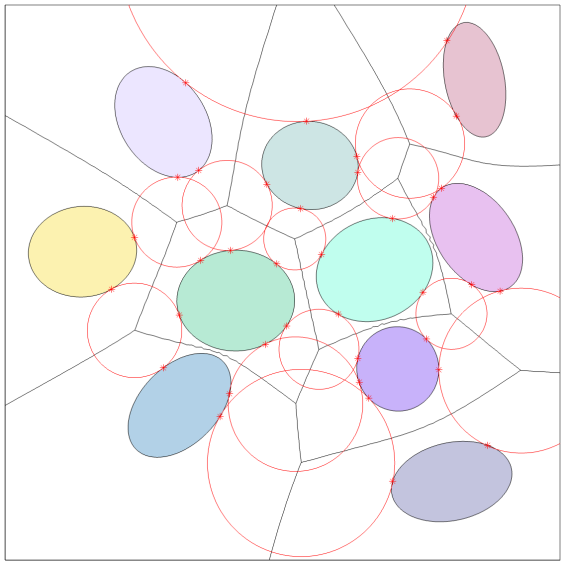

FIGURE 11. Apollonius circles connecting elliptical particles.

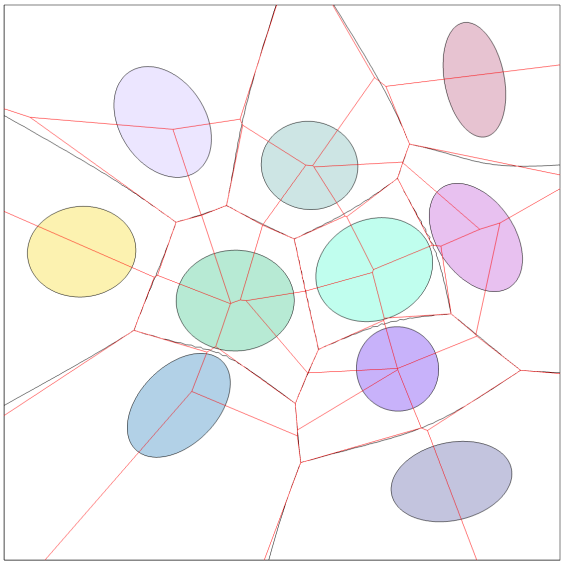

FIGURE 12. Optimized Voronoi structure of elliptic particles before composition.

The result of the system of equations is a polynomial of degree 27. It's still not a simple solution, but it's easy to solve the equations numerically. The resulting circles are shown in the Figure 11 for the same set of particles. The Figure 12 shows the structure and is made up of an average of 6 points per particle. The black line shows the boundaries for particles consisting of 44 points. The structure after composition is shown in red in the Figure 13. There are clear fragments and differences from the exact boundary, but the optimized structure is very consistent even with a large saving of points

5. Conclusion

In this paper, the procedure of structure generation using the LDPM model is presented. It also describes how the structure can be generated using a Voronoi diagram. This procedure relies on the representation of particles by points on their boundary for which the Voronoi diagram is computed. This is followed by a composition of particles for which the structure already corresponds to their shape. Then, a procedure is described on how the algorithm can be optimized using the specific representation. Preliminary results have led us to the conclusion that the specifics are more telling in the construction of the resulting Voronoi diagram and can be used to save a number of points on the particle boundary.

This procedure will be more widely used in the future. It is mainly a matter of trying out additional specific points, then converting the structure to 3D.

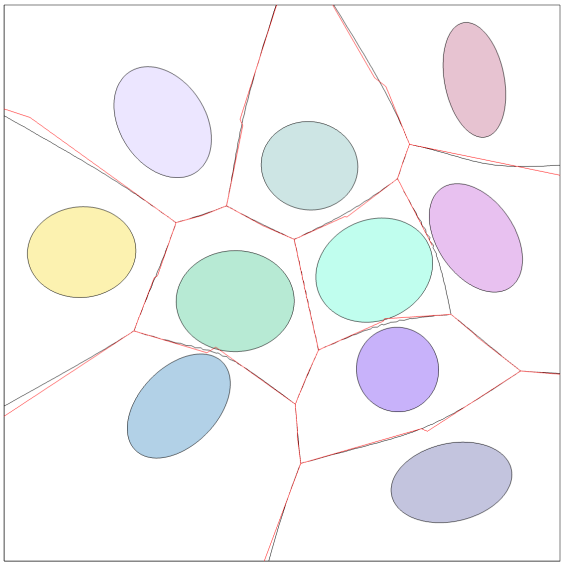

FIGURE 13. Optimized Voronoi structure of elliptic particles after composition.

Acknowledgements

The financial support provided by the GAČR grant No. 21-28525S and by the Czech Technical University in Prague within SGS project with the application registered under the No. SGS20/155/OHK1/3T/11 is gratefully acknowledged.

References

[1] G. Cusatis, A. Mencarelli, D. Pelessone, J. T. Baylot. Lattice Discrete Particle Model (LDPM) for failure behavior of concrete. II: Calibration and validation. *Cement & Concrete Composites* **33**(9):891–905, 2011. MAG ID: 2094226000. `https://doi.org/10.1016/j.cemconcomp.2011.02.010`

[2] F. Aurenhammer. Voronoi diagrams – a survey of a fundamental geometric data structure. *ACM Computing Surveys* **23**(3):345–405, 1991. MAG ID: 1967005434. `https://doi.org/10.1145/116873.116880`

[3] N. Roussel. *Understanding the rheology of concrete.* Elsevier, 2011.

[4] Z. P. Bažant, H. T. Nguyen, A. Abdullah Dönmez. Critical comparison of phase-field, peridynamics, and crack band model M7 in light of gap test and classical

fracture tests. *Journal of Applied Mechanics* **89**(6):061008, 2022. https://doi.org/10.1115/1.4054221

[5] B. L. Karihaloo, A. Carpinteri, M. Elices. Fracture mechanics of cement mortar and plain concrete. *Advanced Cement Based Materials* **1**(2):92–105, 1993. https://doi.org/10.1016/1065-7355(93)90014-F

[6] K. Nagai, Y. Sato, T. Ueda. Mesoscopic simulation of failure of mortar and concrete by 3D RBSM. *Journal of Advanced Concrete Technology* **3**(3):385–402, 2005. https://doi.org/10.3151/jact.3.385

[7] M. Marcon, J. Vorel, K. Ninčević, R. Wan-Wendner. Modeling adhesive anchors in a discrete element framework. *Materials* **10**(8):917, 2017. MAG ID: 2743109236. https://doi.org/10.3390/ma10080917

[8] Q. Du, V. Faber, M. Gunzburger. Centroidal Voronoi tessellations: Applications and algorithms. *Siam Review* **41**(4):637–676, 1999. MAG ID: 2051752778. https://doi.org/10.1137/s0036144599352836

[9] MATLAB. *9.11.0.1837725 (R2021b) Update 2*. The MathWorks Inc., 2021.

[10] I. Z. Emiris, G. M. Tzoumas. Algebraic study of the Apollonius circle of three ellipses. In *EuroCG*, pp. 147–150. 2005.